# The long-term relaxation and build-up transient of photoconductivity in $Si_{1-x}Ge_x$/Si quantum wells



1995 J. Phys.: Condens. Matter 7 4525

(http://iopscience.iop.org/0953-8984/7/23/021)

J. Phys.: Condens. Matter 7 (1995) 4525–4532. Printed in the UK

# The long-term relaxation and build-up transient of photoconductivity in $Si_{1-x}Ge_x$/Si quantum wells

L H Chu†, Y F Chen†, D C Chang‡ and C Y Chang‡

† Department of Physics, National Taiwan University, Taipei, Taiwan

‡ Department of Electronics Engineering and Institute of Electronics, National Chiao Tung University, Hsinchu, Taiwan

Received 20 February 1995, in final form 28 March 1995

**Abstract.** The long-term relaxation and build-up transient of photoconductivity has been observed in $Si_{1-x}Ge_x$/Si quantum wells. The long-term relaxation behaviour of photoconductivity can be described by a stretched-exponential function, $I_{pc}(t) = I_{pc}(0)\exp[-(t/\tau)^{\beta}]$ $(0< \beta <1)$ for $T < 160$ K, which is usually observed in a wide class of disordered materials. The long-term build-up transient of photoconductivity has been measured and formulated at different temperatures, which also indicates the existence of the band-tail states due to alloy disorder. The distribution of tail states has been confirmed to be exponential in energy. Our results suggest that the alloy potential fluctuations induced by compositional fluctuations can strongly influence the transport as well as optical properties of $Si_{1-x}Ge_x$/Si quantum wells.

## 1. Introduction

Considerable experimental and theoretical effort has been directed towards the understanding of the long-term relaxation and build-up transient of photoconductivity, which has been observed in a variety of semiconductors [1]. The long-term relaxation of photoconductivity has been used to study the critical phenomena of transport properties in disordered systems [2]. It is also useful for adjusting the density of a two-dimensional electron gas at a semiconductor interface [3], and can be utilized as a non-destructive method to probe the profile of the impurities in semiconductors [4]. For device applications, it is very detrimental to the operation of modulation-doped field-effect transistors at low temperatures [5]. Several models have been proposed to explain the origin of the long-term relaxation of photoconductivity. Jiang and Lin suggested that the long-term relaxation and build-up transient of photoconductivity in II–VI mixed crystals are caused by the separation of photoexcited carriers by random local-potential fluctuations (RLPF) [2]. Queisser and Theodorou have demonstrated for well defined samples that the spatial separation of photogenerated electrons and holes by a built-in electric field from the macroscopic potential barrier due to band bending at the surface or interfaces leads to long-term relaxation of photoconductivity [5–8]. For layered structures of compound semiconductors, this model predicts an essentially logarithmic photoconductivity decay in time, which is consistent with their experimental observations. The other dominant mechanism involves photoexcitation of electrons from deep level traps which undergo a large lattice relaxation, namely DX centres [9, 10]. In this model, the presence of the long-term relaxation of photoconductivity is because the recapture of electrons by DX centres is prevented by a thermal barrier at low temperatures.

0953-8984/95/234525+08$19.50  

$Si_{1-x}Ge_x$/Si quantum wells have received increasing attention recently because of their potential applications in silicon-based high-speed electronic circuits as well as in new optoelectronic devices. However, the material of the well regions, $Si_{1-x}Ge_x$, belongs to the group of substitutional semiconductor alloys. One of the most important aspects of substitutional semiconductor alloys is the nature of the alloy potential fluctuations that arise from local fluctuations in composition, and hence in the potential energy of the carriers. It has been shown that the alloy potential fluctuations can greatly change the electronic and optical properties of a material: such fluctuations can influence the carrier mobility [11], the profiles of photoluminescence [12] and Raman scattering [13], and the localization of excitons [14]. The occurrence of compositional fluctuations in $Si_{1-x}Ge_x$ alloys has been recognized for a long time [15]. However, studies of the effects of the compositional fluctuations on the electronic and optical properties of $Si_{1-x}Ge_x$ epilayered structures have been rather limited. One of the reasons may be due to the fact that Si/SiGe interface is smeared by Ge surface segregation during growth. Thus, the well resolved band-edge luminescence and the shift of emission with varying well width in $Si_{1-x}Ge_x$/Si quantum wells were only recently reported [16]. Lenchyshyn and co-workers [17] used the concept of compositional fluctuations to explain the existence of the long decay component in their time-resolved photoluminescence spectra of $Si_{1-x}Ge_x$/Si quantum wells. We also used the same mechanism to interpret the anomalous temperature dependence and pumping-power dependence of the photoluminescence spectra [18] in $Si_{1-x}Ge_x$/Si quantum wells. In this paper, we report the observation of the long-term relaxation and build-up transient of photoconductivity in $Si_{1-x}Ge_x$/Si quantum wells. All the results suggest that alloy potential fluctuations induced by compositional fluctuations are responsible for the long-term relaxation and build-up transient of photoconductivity observed here.

## 2. Experiment

$Si_{1-x}Ge_x$/Si strained-layer multiple quantum wells were grown on three-inch diameter (001) Si substrates at 550 °C using a home-made hot-wall multi-wafer ultrahigh-vacuum chemical vapour deposition system. The construction and operation of our system is similar to that which has been reported elsewhere [19]. Prior to growth, the substrate was subjected to a $H_2SO_4 : H_2O_2 = 3 : 1$ clean and a 10% HF dip. The gas sources for Si and Ge were $SiH_4$ and $GeH_4$, respectively. The base pressure of the system was maintained at about $2 \times 10^{-8}$ Torr in the growth chamber. During growth, the system was operated at about 1.0 mTorr. The growth was initiated by depositing a thin Si film of 10 nm thickness. The multiple quantum wells consisted of a total of 20 periods of Si/$Si_{1-x}Ge_x$ layers and a top Si cap layer of about 96 nm. A 10 s growth interruption was employed after each $Si_{1-x}Ge_x$ layer growth while no interruption was used after each Si layer growth. The reason for employing the growth interruption is that the growth rate of $Si_{1-x}Ge_x$ is much higher than that of the Si layer. For Ge atomic mole fraction $x$ of $Si_{1-x}Ge_x$ in Si/SiGe strained multiple quantum wells at about 0.16, the growth rates of Si layers and $Si_{1-x}Ge_x$ layers were about 0.8 nm $min^{-1}$ and 5 nm $min^{-1}$, respectively.

High-resolution double-crystal x-ray diffraction was used to determine the structural quality of these multiple quantum wells. X-ray rocking curves were obtained by using a Philips DCD-3 double-crystal diffractometer. The system was operated in the parallel (+, −) diffraction geometry using $CuK_\alpha$ radiation. A GaAs single crystal with (004) symmetric reflection was used for the first reflection. A dynamical x-ray simulation program was used to aid the determination of the perfection, interfacial abruptness, layer thickness and Ge composition of these multiple quantum wells. Cross sectional transmission electron

microscopy was performed to examine the crystal quality and interfacial abruptness. The crystalline quality of these samples was further checked by high-resolution transmission electron microscopy. Details of the growth technique used and the results of the structural characterization will be published separately [20].

The sample used in the photoconductivity measurements was a $Si_{0.86}Ge_{0.14}$/Si multiple quantum well, with a well width of 200 Å. The same sample has been characterized by photoluminescence measurements, as detailed in a previous report [21]. The obtained energy gap of the quantum well was about 1.03 eV. The ohmic contacts for the lateral conduction measurement were formed on the sample surface by aluminium alloying, which was done by evaporation and then annealing at 300 °C for about 30 min. The dark-room temperature resistance of the sample was about $0.14 \times 10^6\ \Omega$. The sample was attached to a copper sample holder and placed inside a closed-cycle He refrigerator, with care taken to ensure good thermal contact yet electrical isolation. The data at each temperature were taken in such a way that the system was always warmed to room temperature after a measurement and allowed to relax to equilibrium, then cooled down in darkness to the desired temperature of measurements. This was to ensure that the data obtained for each temperature had the same initial condition. In most measurements in this report, a HeNe laser was used as the pumping source, along with a neutral-density filter for obtaining an appropriate photon intensity. A bias of 2.0 V was supplied and the conductivity was measured by a Keithley 236 source measure unit. To confirm that our observed phenomena are not due to the effect of the spatial separation of the electrons and holes created in the Si barrier layer, a pumping source coming from a tungsten lamp dispersed by a monochromator was used and its photon energy was set at the region between the energy gaps of the Si barrier and SiGe well layers.

## 3. Results and discussion

### *3.1. Photoconductivity build-up transient measurements*

A typical example of the dependence of the photoconductivity build-up level on illumination time, with the excitation photon intensity fixed, is shown in figure 1. Figure 2 shows the plot of photoconductivity build-up transients obtained for $Si_{1-x}Ge_x$/Si quantum wells at five different temperatures. The PPC build-up transient curves are normalized by the saturation level $I_{max}$. The dark current has been subtracted.

A striking feature is that the initial transients show a parabolic dependence on illumination time $t$ at low temperatures ($T < 40$ K). As temperature increases above 40 K, the initial transients increase linearly with increasing illumination time. This result is a consequence of the localized-to-delocalized transition caused by the alloy potential fluctuations (APF) in $Si_{1-x}Ge_x$ epilayers, as will be shown below.

According to the analysis in [22], the photoconductivity build-up kinetics can be easily formulated by

$$dn/dt = g - \alpha n \tag{1}$$

where $n$ is the concentration of photogenerated carriers in the conduction band, $g$ is the carrier generation rate and $\alpha$ is the carrier decay rate. From (1), we obtain

$$n(t) = g/\alpha(1 - e^{-\alpha t}). \tag{2}$$

If we assume that the carrier mobility does not depend on carrier concentration $n$, we then have

$$I(t) = I_{max}(1 - e^{-\alpha t}) \tag{3}$$

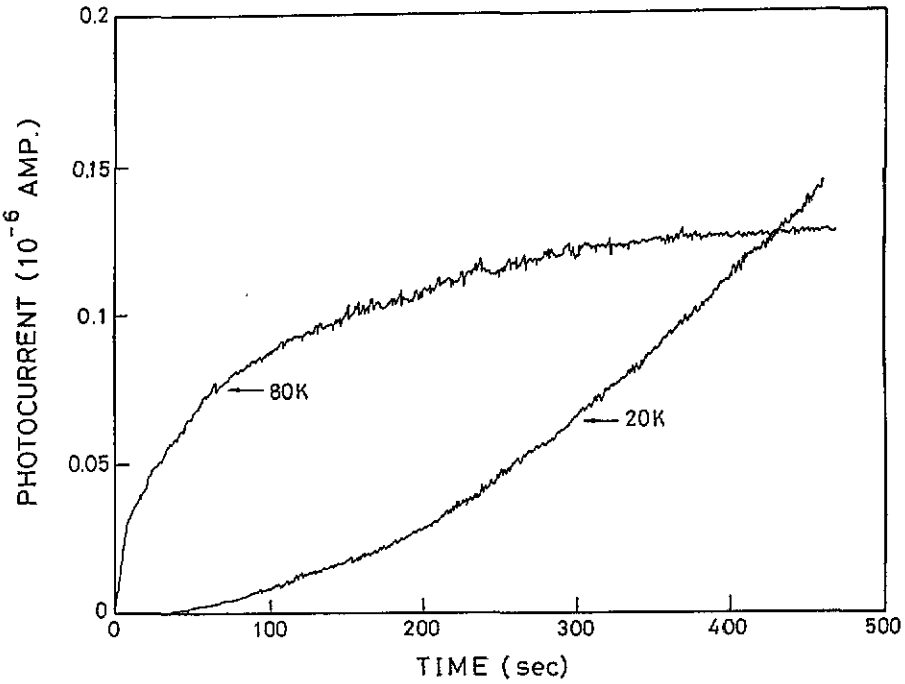


**Figure 1.** Photoconductivity build-up transients as a function of illumination time at 20 K and 80 K.

where $I_{max}$ represents the photoconductivity saturation level. When the sample temperature is high enough, i.e. $T > 40$ K in our case, most of the electrons are above the band edge. In this region, we can consider the carrier mobility to be independent of carrier concentration $n$ as in the above assumption. Figure 3 shows a representative plot of $-\ln(1 - I(t)/I_{max})$ against time at 50 K. The good linear behaviour of the plot demonstrates that the build-up transient is well described by (3). However, when the temperature decreases to below 40 K, the band-edge tail states induced by APF can be used to localize the photoexcited carriers. Thus, the carrier mobility is no longer independent of carrier concentration, and (3) fails to describe the experimental observation. According to the Kubo–Greenwood formula, if we assume that the distribution of the band tail states is exponential in energy, we can obtain [22]

$$I(t) = I_{max}(1 - e^{-\alpha t})^2. \tag{4}$$

For small illumination times, in (4) $I(t)$ has a parabolic time dependence, which is consistent with our experimental results for $T < 40$ K. Figure 4 shows a representative plot of $-\ln[1 - (I(t)/I_{max})^{1/2}]$ against time at 20 K. The linear behaviour of the plot demonstrates that the build-up transient is well described by (4). This result supports the conclusion that the photoconductivity build-up transient is due to the existence of tail states caused by alloy potential fluctuations, which is similar to the observation in II–VI alloys [22, 23].

In figure 2, the full curves are fitted using equation (4) with a constant value of carrier decay rate $\alpha \approx 5.0 \times 10^{-4}\ s^{-1}$ for $T < 40$ K. It reveals that $\alpha$ does not depend on temperature in this temperature region. This result can be explained by the fact that the generated electrons and holes are confined in the localized tail states, and they are spatially separated

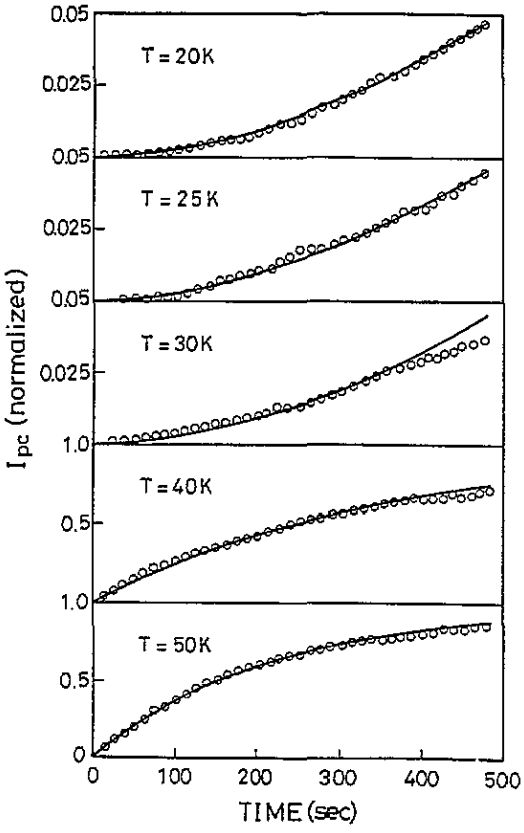


**Figure 2.** Photoconductivity build-up transients for five selected temperatures. Each build-up transient is normalized to unity by the saturation level. The full curves for $T = 20$ K, 25 K and 30 K are fitted by $I(t) = I_{max}(1 - e^{-\alpha t})^2$ and for $T = 40$ K, 50 K by $I(t) = I_{max}(1 - e^{-\alpha t})$.

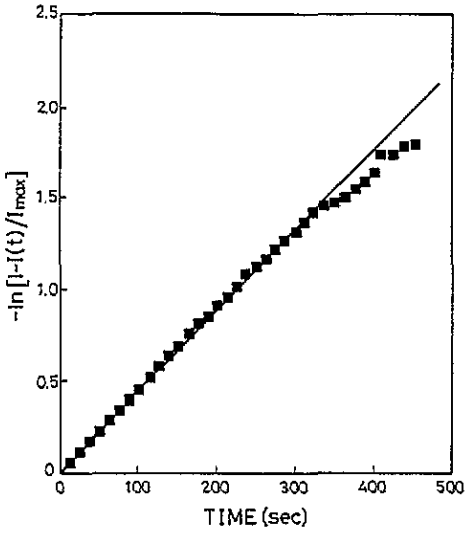


**Figure 3.** Plot of $-\ln(1 - I(t)/I_{max})$ against time at 50 K. The line indicates that the build-up transient is well described by $I(t) = I_{max}(1 - e^{-\alpha t})$.

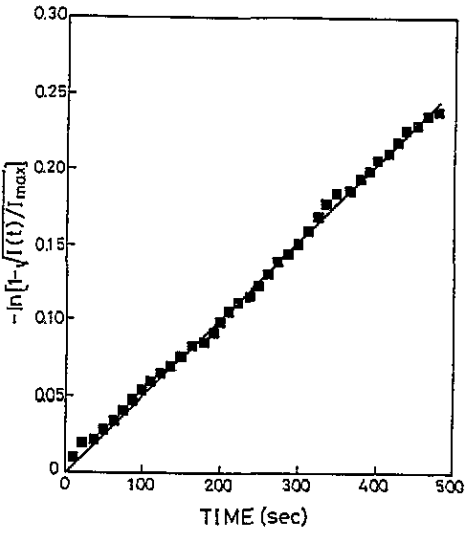


**Figure 4.** Plot of $-\ln[1 - (I(t)/I_{max})^{1/2}]$ against time at 20 K. The line indicates that the build-up transient is well described by $I(t) = I_{max}(1 - e^{-\alpha t})^2$.

in real space. Thus the electrons and holes recombine through the process of quantum tunneling, which does not depend on temperature. For $T > 40$ K, the build-up level achieves the maximum value $I_{max}$ more quickly at higher temperatures, and $\alpha$ tends to increase with increasing temperature for $T > 40$ K. This can be interpreted by the fact that the probability for thermal activation of the localized carriers to overcome the barrier energy caused by APF in $Si_{1-x}Ge_x$ alloys increases with increasing temperature, in the high-temperature region.

In the derivation of (4) we assume that the distribution of the band-tail states caused by APF is exponential in energy. It has been shown that this is the only distribution that can lead to (4) [23]. Thus the exponential tail of states in $Si_{1-x}Ge_x$ alloys is confirmed. Our results, obtained for $Si_{1-x}Ge_x$, are similar to the distribution of the exponential tail of states caused by different disordered systems, such as doped semiconductors, amorphous semiconductors and II–VI alloys. The result may therefore indicate that the exponential tail of states is independent of the origin of the disorder.

### *3.2. Photoconductivity decay measurements*

Photoconductivity decay curves for different temperatures are shown in figure 5. The photoconductivity curves are normalized to unity at $t = 0$, the moment when the excitation light is terminated. The dark current has been subtracted. The decay of photoconductivity in $Si_{1-x}Ge_x$/Si can be approximated by a stretched-exponential function, a behaviour frequently observed in disordered systems [24,25]

$$I_{pc}(t) = I_{pc}(0)\exp[-(t/\tau)^{\beta}] \tag{5}$$

where $\tau$ is the decay time constant and $\beta$ is the decay exponent. This is demonstrated in figure 6 by a plot of $\ln[\ln I_{pc}(0) - \ln I_{pc}(t)]$ as a function of $\ln(t)$ for photoconductivity decay curves obtained at different temperatures. It is clear that linear behaviour is observed. The origin of the stretched-exponential relaxation can be understood by the fact that the rate constant $\nu$ in the decay rate equation is time dependent, i.e.

$$d\Delta/dt = -\nu(t)\Delta. \tag{6}$$

Equation (6) describes the rate of decay for small departures $\Delta$ from equilibrium. A single-valued rate constant $\nu$ will yield the conventional Debye relaxation. Many previous investigations [26–28] showed that if the density of states is exponentially distributed in energy, such as the band-tail states in disordered semiconductors, the rate constant $\nu$ exhibits a power-law time dependence. Inserting a power-law time dependence for $\nu$ into (6) and integrating immediately yields a stretched-exponential function. Thus, stretched-exponential decay reveals similarities between the present system and disordered systems, and implies that the microscopic random potential fluctuations are the origin of the observed long-term relaxation of the photoconductivity effect. From figure 6 we can obtain the stretched-exponential parameters $\tau$ and $\beta$ for different temperatures. The value of $\beta$ is insensitive to the change in temperature. Figure 7 demonstrates the plot of $\ln\tau$ against $1/T$, which shows two distinct temperature regions. The photoconductivity relaxation rate increases in the high-temperature region, and is constant in the low-temperature region. This behavior is similar to that of the carrier decay rate obtained from photoconductivity build-up measurements.

Previously, the long-term photoconductivity relaxation was observed in layered structures of III–V compound semiconductors [29, 30]. The long-term photoconductivity was attributed to the separation of photogenerated electrons and holes by built-in electric fields from the macroscopic barrier due to band bending at surfaces or interfaces. It is

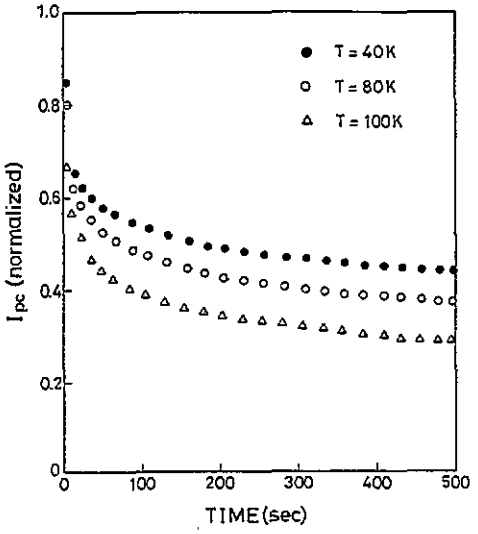


**Figure 5.** Photoconductivity decay curves for three selected temperatures. Each decay curve is normalized to unity at $t = 0$.

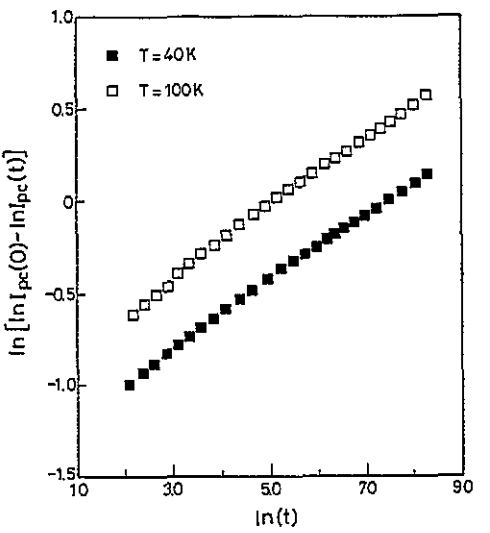


**Figure 6.** Plot of $\ln[\ln I_{pc}(0) - \ln I_{pc}(t)]$ against $\ln t$ for two selected temperatures. The curves indicate that the photoconductivity decays according to the stretched-exponential function, $I_{pc}(t) = I_{pc}(0)\exp[-(t/\tau)^{\beta}]$.

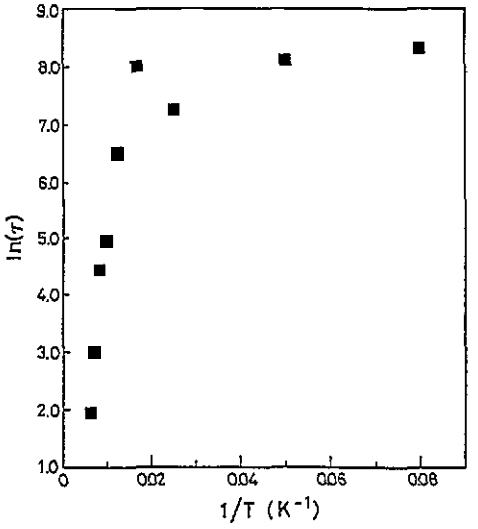


**Figure 7.** Semilogarithmic plot of the decay time constant $\tau$ as a function of $1/T$.

possible that our measured long-term relaxation of photoconductivity may also have the same origin. However, this model predicts a logarithmic photoconductivity decay in time, which is inconsistent with our results. Furthermore, we have set the wavelength of the pumping source such that its photon energy is between the energy gaps of the Si barrier layer and the $Si_{1-x}Ge_x$ well layer. For this wavelength, the photoexcited electrons and holes can only be created in the well region. Under this condition, the long-term relaxation and the build-up photoconductivity transients can still be observed. Thus, the spatial separation of photoexcited electrons and holes due to a macroscopic barrier can be ruled out in the

interpretation of our observed long-term photoconductivity relaxation.

## 4. Conclusions

The long-term build-up and decay of photoconductivity have been investigated in $Si_{1-x}Ge_x/Si$ quantum wells. From an analysis of the kinetics of the photoconductivity measurements, we have shown that the carrier transport properties are strongly influenced by tail states caused by alloy disorder in $Si_{1-x}Ge_x$ epilayers. The distribution of the tail states has been obtained from the photoconductivity build-up measurements and is confirmed to be exponential in energy. The photoconductivity decay profile follows stretched-exponential relaxation, which is commonly observed in disordered systems. The experimental results obtained here, together with previous results obtained from photoluminescence spectra, suggest that the alloy potential fluctuations induced by the compositional fluctuations are very important for the investigation of physical properties and device applications in $Si_{1-x}Ge_x/Si$ quantum wells.

## Acknowledgments

This work was partially supported by the National Science Council of Taiwan.

## References

[1] Sheinkman M K and Shik A Ya 1976 *Fiz. Tekh. Doluprovodn.* **10** 209 (Engl. transl. 1976 *Sov. Phys. Semicond.* **10** 128)
[2] Lin J Y and Jiang H X 1989 *Phys. Rev.* B **40** 10025
[3] Stormer H J, Dingle R, Gossard A C, Wiegmann W W and Sturge M D 1974 *Solid State Commun.* **29** 705
[4] Theodorou D E, Queisser H J and Bauser E 1982 *Appl. Phys. Lett.* **41** 628
[5] Nathan M I 1986 *Solid State Electron.* **29** 167
[6] Queisser H J and Theodorou D E 1979 *Phys. Rev. Lett.* 43, 401
[7] Theodorou D E and Queisser H J 1980 *Appl. Phys.* **23** 121
[8] Queisser H J and Theodorou D E 1986 *Phys. Rev.* B **33** 4027
[9] Lang D V and Logan R A 1977 *Phys. Rev. Lett.* **39** 635
[10] Lang D V, Logan R A and Joros M 1979 *Phys. Rev.* B **19** 1015
[11] Blood P and Grassie A D C 1984 *J. Appl. Phys.* **56** 1866
[12] Singh J and Bajaj K K 1986 *Appl. Phys. Lett.* **48** 1077
[13] Parayanthal P and Pollak F H 1984 *Phys. Rev. Lett.* **52** 1822
[14] Shui Lai and Klein M V 1980 *Phys. Rev. Lett.* **44** 1087
[15] Feldman D W, Ashkin M and Parker J H 1966 *Phys. Rev. Lett.* **17** 1209
[16] Sturm J C, Manoharan H, Lenchyshyn L C, Thewalt M L W, Rowell N C, Noël J P and Houghton D C 1991 *Phys. Rev. Lett.* **66** 1362
[17] Lenchyshyn L C, Thewalt M L W, Houghton D C, Noël J P, Rowell N L, Sturm J C and Xiao X 1993 *Phys. Rev.* B **47** 16655
[18] Chen Y F, Pan S C, Yuang Y S, Chang D C and Chang C Y 1995 *Phys. Rev.* B to be published
[19] Meyerson B S 1986 *Appl. Phys. Lett.* **48** 797
[20] Chang J C, Chang C Y, Jung T G, Tsai W C, Wang P J, Lee J Y and Chen L J (unpublished)
[21] Pan S C, Chen Y F, Chang D C and Chang C Y 1993 *Chin. J. Phys.* **31** 759
[22] Lin J Y, Dissanayake A, Brown G and Jiang H X 1990 *Phys. Rev.* B **42** 5855
[23] Jiang H X, Dissanayake A and Lin J Y 1992 *Phys. Rev.* B **45** 4520
[24] Kakalios J, Street R A and Jackson W B 1987 *Phys. Rev. Lett.* **59** 1037
[25] Chen Y F, Huang S F and Chen W S 1991 *Phys. Rev.* B **44** 12748
[26] Campos M, Giacometti J A and Silver M 1979 *Appl. Phys. Lett.* **34** 226
[27] Jackson W B 1988 *Phys. Rev.* B **38** 3595
[28] Crandall R S 1991 *Phys. Rev.* B **43** 4057
[29] Oueisser H J 1985 *Phys. Rev. Lett.* **54** 234
[30] Schubert E F, Fischer A and Ploog K 1985 *Phys. Rev.* B **31** 7937